Path-Integral Calculation of the Mean Number of Overcrossings in an Entangled Polymer Network

Gustavo A. Arteca†

Département de Chimie et Biochimie, Laurentian University, Ramsey Lake Road, Sudbury, Ontario, Canada P3E 2C6, and Department of Physical Chemistry, Uppsala University, Box 532, S-751 21 Uppsala, Sweden

Received August 28, 1998

A quantitative characterization of entanglements between polymer chains is essential for understanding the behavior of polymer solutions. When dealing with unknotted open chains, that characterization must rely on *geometrical* (rather than topological) measures of entanglement complexity. In this work, we deal with a simple geometrical shape descriptor: the *mean overcrossing number* of a set of curves. This descriptor provides a physically intuitive characterization of self-entanglements in a chain or entanglements in a network. Many of the analytical properties of the mean overcrossing number are still not well understood. In part, this is due to the use of numerical algorithms for its computation. Path-integral formalisms offer an improvement over this situation, by providing analytical expressions for the geometrical descriptors or, at least, more efficient algorithms for their evaluation. In this work, we discuss an approach to represent overcrossing numbers by path integrals. The formalism is general enough to be applied to polymer networks. In the particular case of networks on the cubic lattice, we provide a set of closed formulas for the fast (exact) calculation of the mean overcrossing number. By using our methodology, it is now possible to perform efficient analyses of entanglement complexity in polymer solutions modeled by computer simulations on lattices. Our results can be used to gain a better understanding of the dynamical behavior of entangled polymers.

INTRODUCTION

Rheological and dynamical properties of polymer melts and concentrated polymer solutions can be explained by the occurrence of *entanglements*, caused by polymer chains interpenetrating each other (or themselves) strongly.[1,2] In the absence of enzymes, bonds cannot physically "cross through" one other to remove these entanglements. As a result, chain motions become *geometrically or topologically constrained*. This feature confers to polymer melts a blend of both viscous and elastic properties. A microscopic picture of these motions is provided by the "reptation" hypothesis,[1,3] whereby polymer chains under a shear flow unentangle by slowly slithering away past each other. Recent direct observations of conformational dynamics have confirmed this model.[4−6]

Entanglements can be "trapped" by closing a chain and forming a knot. Similarly, entanglements between two or more chains can be trapped by forming links after closure. This situation is found in circular DNA,[7,8] where entanglements can be characterized by a number of *topological invariants*, such as linking numbers[9−11] or descriptors of knot type.[12,13] Most commonly, however, one deals with entanglements (or *self-entanglements*) between *open chains*. In this case, chains do not have topological constraints but their dynamical behavior is still dictated by the impossibility of dislogding local entanglements instantaneously. As a result, over a period of time chains are effectively entangled within their loops or the loops of neighboring chains. However, since open chains are topologically trivial, the characterization of these entanglements requires *geometrical*, rather than topological, measures. A great deal of work has been devoted recently to the development of geometrical measures of entanglement complexity. In this work, we present and discuss an efficient method to compute the *mean overcrossing number*, which provides a detailed geometrical description of self-entanglements in a polymer network.

The mean overcrossing number (or "average crossing number"), denoted by $\overline{N}$, is a convenient descriptor of polymer shape.[14−16] It can be defined in chains with and without branching,[17] as well as in transient polymer networks.[18] Its intuitive definition is very simple. For an instantaneous ("frozen") polymer configuration, $\overline{N}$ measures the number of bond−bond crossings in a regular *two-dimensional projection* of the chain, averaged over all possible projections. Figure 1 provides a simple illustration of this idea. It shows a short chain in the cubic lattice, comprising six "bonds" C_i, $i \leq 6$. In the top presentation, the chain exhibits one "overcrossing" ($N = 1$), where C_2 is over C_6 along the line of sight. When this polymer is rigidly rotated, it may appear to exhibit a *maximum* of $N = 2$ overcrossings (right below) or a *minimum* of $N = 0$ overcrossings (left below). When all the spatial directions are taken into account, the average $\overline{N}$ result is in general a noninteger. (As we show below, the *exact* result for this particular chain is $\overline{N} = 1/2$.)

† Permanent address: Département de Chimie et Biochimie, Laurentian University, Ramsey Lake Road, Sudbury, Ontario, Canada P3E 2C6. E-mail: Gustavo@nickel.laurentian.ca.

10.1021/ci980144l CCC: $18.00
Published on Web 05/01/1999

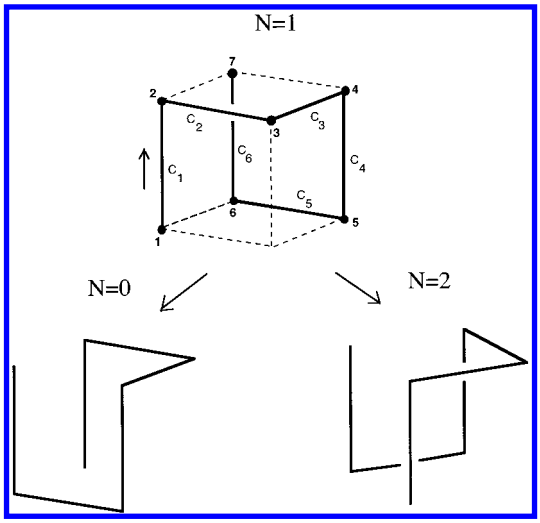

Figure 1. Examples of regular projections with various overcrossing numbers in a small polygon in the cubic lattice. (The *exact* mean overcrossing number for this polygon is $\overline{N} = 1/2$.)

The usefulness of geometrical measures of entanglement (which include also writhe,[9,19−24] torsion,[25] and knot energies[26−31]) has been demonstrated by a number of experimental observations on closed molecular chains. Recent work shows that the mean overcrossing number of the "canonical" conformation of a given mathematical knot correlates linearly with the actual electrophoretic diffusion velocity of DNA in the same knot.[32,33] (A knotted tube of *fixed* length is in its canonical or "ideal" conformation when it has the maximum possible uniform diameter.[34]) In addition, the time-averaged mean number of overcrossings (denoted by $\langle\overline{N}\rangle$) is found to be proportional to the $\overline{N}$ value for the canonical conformer. These results suggest that, although $\overline{N}$ is a geometric property, it can be related to *the dynamical consequences of the topological entanglements in a polymer*. In other words, $\langle\overline{N}\rangle$ behaves as a "weak" topological invariant, allowing some degree of discrimination for classifying knots.[32−34] Similar correlations between knot complexity and the writhe have also been discussed in the literature.[35] In contrast, much less is known about the geometrical descriptors for *open* (unknotted) *chains*. In this work, we contribute to advancing this field, by studying the mean number of overcrossings in a melt of chains with arbitrary topology.

Recent work has begun to uncover some of the key properties of $\overline{N}$ in *single* open chains. From the static viewpoint, it has been established that the *configurationally* (or time-averaged) mean overcrossing number exhibits scaling with the number of connected monomers, n. Results show a power-law of the form $\langle\overline{N}\rangle \approx n^{\beta}$, although the critical exponent is not rigorously known. Recent work on the value of this exponent indicates (a) an upper bound $\beta = 1.33 \pm 0.03$ from the analysis of medium-size off-lattice chains with excluded volume,[36] (b) a lower bound $\beta = 1.12 \pm 0.01$ from long-chain lattice polygons,[21] (c) a conjectured estimate $\beta \leq 1.4$ using a path-integral argument,[23,37] (d) an effective value $\beta = 1.4 \pm 0.1$ in native states of medium-size compact proteins,[36] and (e) a rigorous bound $1 < \beta \leq 4/3$ for knots in canonical configurations.[38,39] From the dynamic viewpoint, fluctuations in $\langle\overline{N}\rangle$ are found to accompany some configurational transitions.[40−44] These changes in $\langle\overline{N}\rangle$ provide important information on molecular shape not readily available from other descriptors (*e.g.*, molecular size).

In polymer melts, the static and dynamic behavior of $\langle\overline{N}\rangle$ is still unknown. Treating these systems is difficult for two reasons. Firstly, overcrossings are computed normally by algebraic techniques based on regular projections. These techniques are not very efficient computationally. Without improved algorithms, it is difficult to tackle the case of polymer networks, where the number of overcrossings is expected to grow fast. Secondly, algebraic methods do not lead to analytical formulas for $\langle\overline{N}\rangle$.

In this work, we propose an improved approach for the analysis of mean overcrossing numbers in general polymer networks. The method is based on a path integral representation for $\overline{N}$, originally developed for *closed* loops. Here, we generalize the technique to the case of *an ensemble of open curves*. Our formulation contains the lattice polymer models[45,46] as a particular case. These models have been used in many applications, including the study of polymer melts and networks[47,48] as well as protein stability and folding mechanisms.[49,50] Here, we provide a complete set of closed formulas for the computation of $\overline{N}$ in the case of polymer networks defined on a cubic lattice.

The work is organized as follows. In the next section, we discuss the derivation of the general path-integral equations for the computation of $\overline{N}$. The approach uses a number of ideas from differential geometry of Gauss maps. Our discussion provides all the background needed to follow the derivation. Another section applies these results to the case of the cubic lattice. The formulas are tested in a number of examples, one of which resembles a lattice model of a compact polymer melt. Conclusions and further comments are found in the last section.

ANALYTICAL COMPUTATION OF $\overline{N}$ VIA PATH INTEGRALS

The numerical evaluation of $\overline{N}$ for a generic chain or network polymer (either on a lattice or an off-lattice continuum) is computationally quite demanding. The simplest approach is as follows:[16] (i) enclose the polymer by the smallest sphere (centered at its geometrical center); (ii) choose a random point $\mathbf{r}$ on the sphere and then project the chain to a plane tangent to the sphere at $\mathbf{r}$; (iii) compute the number of bond−bond overcrossings (N) on the projected image; and (iv) repeat the procedure for a large number of randomized projections on the sphere. If we denote by m_N the number of projections (over a total of m) that exhibit N overcrossings, the mean overcrossing number becomes

$$\overline{N} = \lim_{m\to\infty} \sum_{N=0}^{\max N} N\frac{m_N}{m} \qquad (1)$$

The evaluation of $\overline{N}$ uses the positions of the monomer "beads" and the connectivity table for the bonds. In a random (not fully connected) network containing n beads (*i.e.*, with $O(n)$ bonds), the evaluation of eq 1 requires one to check $O(n^2)$ possible bond−bond crossings. (In a linear chain, *max* $N = (n-2)(n-3)/2$.) Thus, the direct computation of $\overline{N}$ by

random projections becomes CPU-intensive as the size of the system increases. In addition, a nonanalytical approach produces few insights on exact properties of $\overline{N}$.

Analytical measures of entanglement are known in polymer theory for some chain topologies. For instance, the *Gauss linking number*[10,51,52] and the *writhe*[9,11] can be written as line integrals, and they provide a nonalgebraic characterization for links and knots in entangled closed curves,[1,53−57] as well as some properties of self-avoiding walks.[22−24] By using the Gauss "loop" integral[9,52] and spherical maps,[58] the mean overcrossing number of closed loops can also be rendered as a path integral.[59−61] Recently, this technique has been used to study the relation between overcrossing numbers and knot energies in polymer rings[28,60−62] and the scaling behavior of $\overline{N}$ with the number of monomers in *single* chains.[23,37] In this section, we show how this approach can be extended to produce a measure of *self-entanglements* in a general polymer network.

For the present formulation, we will consider a general form of a polymer network. The network will be defined by n "beads" (or "monomers") and a connectivity matrix. Let us consider n identical beads, each defined by a position vector $\mathbf{r}_i$, $i = 1, 2, ..., n$. The connectivity matrix establishes how these monomers are joined by segments. In the most general case, we assume that these segments *are curved*. Let the curve γ_i ($i \leq n-1$) describe the "segment" joining monomers i and $i+1$, according to some arbitrary ordering. Each segment is a parametrized path over the unit interval I=[0,1]

$$\gamma_i: \quad I \rightarrow R^3, \quad \gamma_i(0) = \mathbf{r}_i, \quad \gamma_i(1) = \mathbf{r}_{i+1} \tag{2}$$

with Cartesian coordinates $\gamma_{i1} = x_i(s)$, $\gamma_{i2} = y_i(s)$, and $\gamma_{i3} = z_i(s)$ for a generic position vector $\gamma_i(s) = \sum_{m=1}^{3} \gamma_{im}\mathbf{e}_m$ and continuous parametric derivatives $\dot{\gamma}_i(s) = \partial\gamma_i(s)/\partial s$, $\forall s \in I$, so that

$$\dot{\gamma}_i(0) = \lim_{s\downarrow 0} \dot{\gamma}_i(s), \quad \dot{\gamma}_i(1) = \lim_{s\uparrow 1} \dot{\gamma}_i(s) \tag{3}$$

The set of all points in the segment (*i.e.*, the image of the map γ_i) will be indicated by G_i:

$$G_i = \{\gamma_i(s) \in R^3, s \in I\} \tag{4}$$

A curved segment can be used when describing a wormlike (or Kratky−Porod) polymer model. In lattice or off-lattice polymer models defined by standard chemical bonds, the segments will be straight lines. In this case, we shall use C_i instead of G_i:

$$C_i = \{\gamma_i(s) \in R^3: \ \gamma_i(s) = \mathbf{r}_i + s\,(\mathbf{r}_{i+1} - \mathbf{r}_i),\ s \in I\} \tag{5}$$

Let us consider now the average number of "bond−bond" overcrossings associated *exclusively* with the projections of only two segments, G_i and G_j. This contribution to the mean overcrossing number will be indicated as $\overline{N}(G_i,G_j)$. Two such generic (curved) segments appear in the left-hand side of Figure 2. To derive an analytical expression for $\overline{N}(G_i,G_j)$, we will adapt the techniques developed in refs 23, 43, and 59−61 for the study of closed curves to the present case of overcrossings between open segments in a network. The derivation uses simple concepts from differential geometry,

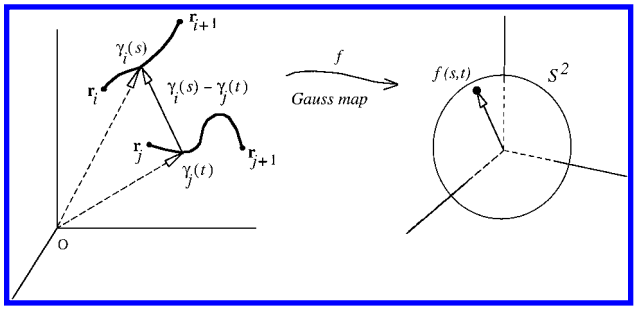

Figure 2. Notion of a Gauss map defined between two generic overcrossing segments G_i and G_j and the unit 2-sphere S^2. (The G_i and G_j segments are represented by the parametrized paths $\gamma_i(s)$ and $\gamma_j(t)$, respectively. When "viewed" along the direction of the vector $\gamma_i(s) - \gamma_j(t)$ indicated, the two segments exhibit one overcrossing.)

in particular, some notions related to the theory of the *degree* of a Gauss map.[63] For completeness, we give a detailed discussion below.

To understand first the integral formulation intuitively, we can see in simple geometrical terms *when* an overcrossing takes place between two general segments. Figure 2 shows two curved segments G_i and G_j; they can be part of a network or simply sections of a longer polymer. Let us assume that, in a random projection, the segment G_i overcrosses G_j at a single point. As indicated in Figure 2, the overcrossing will be defined by the points $\gamma_i(s) \in G_i$ and $\gamma_j(t) \in G_j$. The occurrence of this "crossing" implies that the difference vector $\gamma_i(s) - \gamma_j(t)$ *coincides with the "line of sight" for the projection*. (That is, $\gamma_i(s) - \gamma_j(t)$ is perpendicular to a plane tangent to the smallest sphere enclosing the network.) Consider now a *general projection,* defined by a point $\mathbf{p}$ on the surface of the sphere enclosing the system, where $\mathbf{p}$ is measured from the center of that sphere. We can then see that this projection will have a number of overcrossings (N) *equal to the number of difference vectors of the type* $\gamma_i(s) - \gamma_j(t)$ *that are parallel to* $\mathbf{p}$. In other words, the number of overcrossings associated with a given line of sight $\mathbf{p}$ can be computed from the number of elements (or cardinality) of the mapping between $\gamma_i(s) - \gamma_j(t)$ vectors and a point $\mathbf{p}$ on the unit sphere, for some i, j, s, and t. Thus, the mean number of overcrossings can be obtained by integrating the cardinality of this map over all points $\mathbf{p}$ on the unit sphere.

Quantitatively, we proceed as follows. Let f be a Gauss (or "spherical") map[58,63]

$$f: \ I \times I \rightarrow S^2 \tag{6}$$

from a pair of points on curves parametrized over the unit interval I, onto the unit 2-sphere S^2 (see Figure 2). For two curves G_i and G_j, the simplest such mapping is

$$f_{ij}(s,t) = \frac{\gamma_i(s) - \gamma_j(t)}{||\gamma_i(s) - \gamma_j(t)||} \in S^2 \subset R^3 \tag{7}$$

with components:

$$f_{ij}(s,t) = \sum_{k=1}^{3} f_{ij}^{(k)}\mathbf{e}_k, \quad f_{ij}^{(1)} = \frac{x_i(s) - x_j(t)}{||\gamma_i(s) - \gamma_j(t)||}, \quad \text{etc.} \tag{8}$$

The number of overcrossings N_p associated with a projection $\mathbf{p} \in S^2$ is given as $N_p = card\{f^{-1}(\mathbf{p})\}$. Formally, the mean

number of overcrossings can then be calculated by integrating on S^2

$$\overline{N}(G_i,G_j) = \int_{S^2} card\{f^{-1}(\mathbf{p})\}d\sigma \Big/ \int_{S^2} d\sigma \qquad (9)$$

where $d\sigma$ is the surface differential (or volume element on S^2) at $\mathbf{p}$, *i.e.*

$$\int_{S^2} d\sigma = 4\pi$$

By integrating over 2-forms,[54,59] the denominator in eq 9 can be computed in two equivalent ways. Either one integrates the absolute value of $d\sigma$ over the image of the mapping f on S^2, or one integrates the reciprocal image of f on the domain $I \times I$

$$\overline{N}(G_i,G_j) = \frac{1}{4\pi}\int_{f(I\times I)} |d\sigma| = \frac{1}{4\pi}\int_{I\times I} |f*d\sigma| \qquad (10)$$

where $f*d\sigma$ stands for the "pullback" (or "reciprocal image") of the volume element $d\sigma$ under map f. The second integral provides the best approach, because it transforms $\overline{N}(G_i,G_j)$ into a *path integral* over parametric curves. (In this formulation, $\overline{N}(G_i,G_j)$ *resembles* the degree of the map f. However, $\overline{N}(G_i,G_j)$ is *not* a degree since the integrand in eq 10 is *always* positive.[63]) Quantitatively, the computation of the pullback is accomplished by representing $d\sigma$ in terms of "exterior" derivatives of the map f along the paths γ_i and γ_j. These derivatives, usually denoted by $f*\dot{\gamma}_i$ and $f*\dot{\gamma}_j$, "weigh" the differential $d\sigma$ in terms of the curvature of f. In this representation, $\overline{N}(G_i,G_j)$ in eq 10 becomes a double line integral of the pullback along the parametrized segments $\gamma_i(s)$ and $\gamma_j(t)$:

$$\overline{N}(G_i,G_j) = \frac{1}{4\pi}\int_{I\times I} |d\sigma(f*\dot{\gamma}_i, f*\dot{\gamma}_j)|\, ds\, dt \qquad (11)$$

The exterior derivatives are defined in terms of a mapping $f*_{(\mathbf{p})}$ relating tangent spaces ($T(I\times I) \rightarrow T(S^2)$). In practice, we they are computed as[58]

$$f*\dot{\gamma}_i = \sum_{k=1}^{3}\sum_{m=1}^{3} \dot{\gamma}_{im}\frac{\partial \mathbf{f}_{ij}^{(k)}}{\partial \gamma_{im}}\mathbf{e}_k, \quad \text{for some } s, t \qquad (12)$$

The vectors $f*\dot{\gamma}_i$ and $f*\dot{\gamma}_j$ define a plane that is tangent to the unit sphere. Accordingly, a vector $f*\dot{\gamma}_i \times f*\dot{\gamma}_j$ will be perpendicular to the tangent plane, and its norm will be proportional to the differential of surface. Since $f_{ij}(s,t)$ is a unit vector normal to S^2 (and pointing *away* from S^2), the "weighed" surface differential in eq 11 becomes the scalar

$$d\sigma(f*\dot{\gamma}_i, f*\dot{\gamma}_j) = -f_{ij}\cdot(f*\dot{\gamma}_i \times f*\dot{\gamma}_j) \qquad (13)$$

To evaluate eq 13, we use the cartesian derivatives of the Gauss mapping $f_{ij}(s,t)$ as indicated in eq 12. For example, for the x_i-coordinate we have

$$\frac{\partial f_{ij}^{(1)}}{\partial x_i} = \frac{1}{||\gamma_i - \gamma_j||} - \frac{(x_i - x_j)^2}{||\gamma_i - \gamma_j||^3} \qquad (14a)$$

$$\frac{\partial f_{ij}^{(2)}}{\partial x_i} = -\frac{(x_i - x_j)(y_i - y_j)}{||\gamma_i - \gamma_j||^3} \qquad (14b)$$

$$\frac{\partial f_{ij}^{(3)}}{\partial x_i} = -\frac{(x_i - x_j)(z_i - z_j)}{||\gamma_i - \gamma_j||^3} \qquad (14c)$$

for some s and t. Similar expressions hold for the Cartesian coordinates y and z. After replacing in eq 12, we obtain the exterior derivatives:

$$f*\dot{\gamma}_i = \frac{\dot{\gamma}_i}{||\gamma_i - \gamma_j||} - \frac{(\gamma_i - \gamma_j)}{||\gamma_i - \gamma_j||^3}\{\dot{\gamma}_i\cdot(\gamma_i - \gamma_j)\} \qquad (15a)$$

$$f*\dot{\gamma}_j = -\frac{\dot{\gamma}_j}{||\gamma_i - \gamma_j||} + \frac{(\gamma_i - \gamma_j)}{||\gamma_i - \gamma_j||^3}\{\dot{\gamma}_j\cdot(\gamma_i - \gamma_j)\} \qquad (15b)$$

Using standard vectors properties (*e.g.*, $\mathbf{a}\times\mathbf{a} = \mathbf{0}$, $\mathbf{a}\cdot(\mathbf{b}\times\mathbf{c}) = (\mathbf{a}\times\mathbf{b})\cdot\mathbf{c}$), eq 13 becomes

$$-f\cdot(f*\dot{\gamma}_i \times f*\dot{\gamma}_j) = \frac{(\gamma_i - \gamma_j)\cdot(\dot{\gamma}_i \times \dot{\gamma}_j)}{||\gamma_i - \gamma_j||^3} \qquad (16)$$

from where we obtain the contribution to $\overline{N}$ due to the segment γ_i overcrossing γ_j:

$$\overline{N}(G_i,G_j) = \frac{1}{4\pi}\int_0^1\int_0^1 \frac{|(\dot{\gamma}_i(s)\times\dot{\gamma}_j(t))\cdot(\gamma_i(s) - \gamma_j(t))|}{||\gamma_i(s) - \gamma_j(t)||^3}\, ds\, dt \qquad (17)$$

Equation 17 is the main ingredient for our analysis. Note that this formula describes the situation where γ_i crosses *over* γ_j (cf. eq 7). Of course, the crossings where γ_j is over γ_i will produce an identical contribution. Note that eq 17 provides the *self-overcrossings* within a given segment, if the integrals are taken to be both along the *same* γ_i path.

We can now compute the mean overcrossing number of an *entire network*, as defined by *all possible* $\{G_i\}$ *segments*, $G = \cup_{i=1} G_i$. This number, denoted by $\overline{N} = \overline{N}(G,G)$ involves *all* combinations of segment−segment overcrossings, including all possible pairs of segments as well as segment *self*-overcrossings. The total value is

$$\overline{N} = \overline{N}(G,G) = 2\sum_i\sum_{j>i}\overline{N}(G_i,G_j) + \sum_i \overline{N}(G_i,G_i) \qquad (18)$$

where the diagonal terms $\overline{N}(G_i,G_i)$ represent the self-overcrossings.

Equation 18 is simplified if one considers a network C formed by straight line segments, *e.g.*, a lattice. In this case,

the network is defined by $C = \cup_{i=1} C_i$, where each segment satisfies eq 5. Since straight-line segments cannot overcross with themselves, the diagonal terms in eq 18 will vanish in a lattice. Finally, we obtain our main result

$$\overline{N}_{\text{lattice}} = \overline{N}(C,C) = \frac{1}{2\pi} \sum_i \sum_{j>i} \int_0^1 \int_0^1 \frac{|(\dot{\gamma}_i(s) \times \dot{\gamma}_j(t))\cdot(\gamma_i(s) - \gamma_j(t))|}{||\gamma_i(s) - \gamma_j(t)||^3} ds\, dt \tag{19}$$

where the *i, j* indices run over *distinct* segments.

Equation 19 provides an analytical representation of self-entanglements in a network made of connected straight-line segments. In practice, eq 19 simplifies even further in a lattice: the *i,j*-sums actually *exclude* adjacent segments directly connected by a vertex, since the latter cannot overcross. This is always the case in a single polymer chain defined by $n - 1$ sequentially connected segments. In this case, eq 19 becomes[43]

$$\overline{N}_{\text{single chain}} = \frac{1}{2\pi} \sum_{i=1}^{n-3} \sum_{j=i+2}^{n-1} \int_0^1 \int_0^1 \frac{|(\dot{\gamma}_i(s) \times \dot{\gamma}_j(t))\cdot(\gamma_i(s) - \gamma_j(t))|}{||\gamma_i(s) - \gamma_j(t)||^3} ds\, dt \tag{20}$$

Further simplifications can be achieved by using the lattice symmetry, as shown below.

COMPUTATION OF OVERCROSSINGS IN THE CUBIC LATTICE

Here, we analyze a polymer network defined by a series of segments embedded in a cubic lattice. Lattice symmetry provides a simple classification for those bonds contributing to overcrossings: *the only segments that can overcross are those that are perpendicular to each other and noncoplanar*. Note that connected segments in the cubic lattice do not overcross, neither do parallel, colinear, or coplanar segments. Thus, we only need to study the case of two perpendicular segments displaced along a lattice direction.

Consider, without loss of generality, two noncoplanar segments C_1 and C_3 displaced along the *y*-direction, in a cubic lattice with lattice spacing *b*. Let C_1 be parallel to the *z*-direction, defined by vectors (connected "beads" or lattice nodes) $\mathbf{r}_1 = (x_1,y_1,z_1)$ and $\mathbf{r}_2 = (x_2,y_2,z_2) = (x_1,y_1,z_1+b)$. Let C_3 be parallel to the *x*-direction, defined by vectors $\mathbf{r}_3 = (x_3,y_3,z_3)$ and $\mathbf{r}_4 = (x_4,y_4,z_4) = (x_3+b,y_3,z_3)$. As a result, we have the following parametrized paths and path derivatives:

$$\gamma_1(s) = (x_1,y_1,z_1 + sb), \quad \dot{\gamma}_1 = (0,0,b) \tag{21a}$$

$$\gamma_3(t) = (x_3 + t\,b,y_3,z_3), \quad \dot{\gamma}_3 = (b,0,0) \tag{21b}$$

Note that, in order to produce overcrossings, C_1 and C_3 cannot be coplanar, that is $y_1 \neq y_3$. Using eq 21, we obtain $|(\dot{\gamma}_1 \times \dot{\gamma}_3)\cdot(\gamma_1 - \gamma_3)| = |y_1 - y_3|b^2$. Finally, eq 17 gives us the expression for the mean overcrossing number $\overline{N}(C_1,C_3)$:

$$\overline{N}(C_1,C_3) = \frac{|y_1 - y_3|b^2}{4\pi} \int_0^1 \int_0^1 [(x_3 + tb - x_1)^2 + (y_1 - y_3)^2 + (z_1 + sb - z_3)^2]^{-3/2} ds\, dt =$$

$$\frac{1}{4\pi} \left| \int_{\frac{x_1 - x_3}{y_1 - y_3}}^{\frac{x_1 - x_3 - b}{y_1 - y_3}} \int_{\frac{z_1 - z_3}{y_1 - y_3}}^{\frac{z_1 - z_3 - b}{y_1 - y_3}} [1 + s^2 + t^2]^{-3/2} ds\, dt \right| \tag{22}$$

After evaluating the integral 22,[64] we obtain a simple closed-form expression for $\overline{N}$ written in terms of the coordinates of the four points involved

$$\overline{N}(C_1,C_3) = \frac{1}{4\pi} \left| \arctan\frac{(x_2 - x_4)(z_2 - z_4)}{(y_2 - y_4)d_{24}} - \arctan\frac{(x_2 - x_3)(z_2 - z_3)}{(y_2 - y_3)d_{23}} - \arctan\frac{(x_1 - x_4)(z_1 - z_4)}{(y_1 - y_4)d_{14}} + \arctan\frac{(x_1 - x_3)(z_1 - z_3)}{(y_1 - y_3)d_{13}} \right| \tag{23}$$

where d_{ij} indicates the distance between the *i* and *j* beads. Equation 23 is quite useful because it reveals the structure of the mean overcrossing number $\overline{N}(C_1,C_3)$ between two arbitrary segments in the cubic lattice. As discussed, this equation corresponds to the case of segments C_1 and C_3 displaced along the *y*-direction. If the overcrossing segments were displaced along the *x*-direction, the corresponding $\overline{N}(C_1,C_3)$ value is obtained by exchanging the roles of "*x*" and "*y*" in eq 23. Similarly, if the segments were displaced along the *z*-direction, we only need to exchange the roles of "*z*" and "*y*" in eq 23.

The result (23) can be applied to any pair of overcrossing segments (*i.e.*, perpendicular and noncoplanar "bonds" in the lattice) by simply knowing the coordinates and connectivity of the four lattice nodes involved. With eqs 19 and 23, we can finally compute total number of overcrossings of the network:

$$\overline{N} = \overline{N}_{\text{network}} = 2 \sum_i \sum_{j>i} \overline{N}(C_i,C_j) \tag{24}$$

These formulas can now be tested in simple networks, and their performance compared with the numerical evaluation of overcrossings by using random projections.

Figure 3 shows four different networks defined within the unit lattice cube. In all cases, the overcrossing bonds are separated by *one* lattice distance ($b = 1$). Example I in Figure 3 is made of two disjoint "polymers," examples II and III are single open polymers, whereas example IV is a closed loop. (Example II is also the lattice polymer displayed in Figure 1.) Note that all of networks have similar shape features with respect to molecular size and anisometry;[40-42] they can only be distinguished effectively by measuring their entanglement properties.

In order to compute the total value of $\overline{N}$ for the cases in Figure 3, we only need the contribution to the mean

Table 1. Evaluation of Mean Overcrossing Numbers and Overcrossing Probabilities for the Test Polygons Shown in Figure 3

			individual overcrossing probabilities		
case	$\overline{N}$(exact)	$\overline{N}$(numerical)	A_0	A_1	A_2
I	1/4	0.2501 ± 0.0008	0.8334 ± 0.0006	0.0831 ± 0.000	0.0835 ± 0.0002
II	1/2	0.4998 ± 0.0005	0.5834 ± 0.0004	0.3333 ± 0.0005	0.0833 ± 0.0002
III	2/3	0.6667 ± 0.0005	0.3333 ± 0.0005	0.6667 ± 0.0005	
IV	1	0.999998 ± 0.000002	$(1.4 \pm 0.2) \times 10^{-5}$	0.999974 ± 0.000003	$(1.2 \pm 0.2) \times 10^{-5}$

[a] Numerical results have been obtained by averaging over 10 independent sets calculations, each involving 10^6 random projections. The error bars correspond to one standard deviation. Exact results are derived by using the present eq 23 and 24.

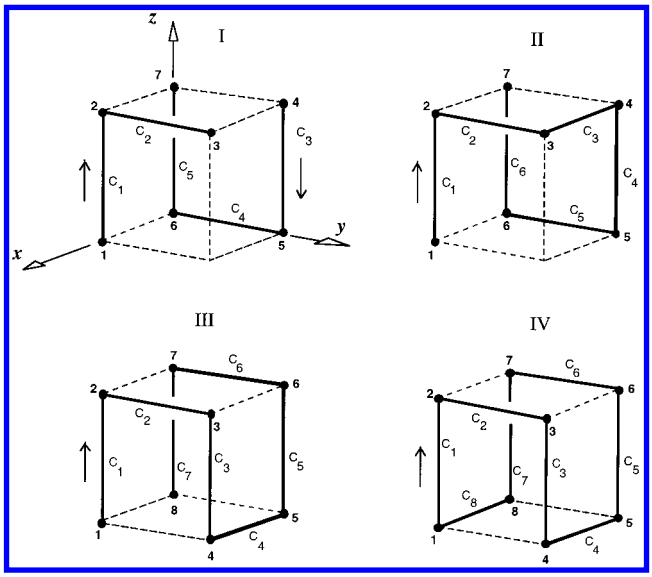

Figure 3. Examples of lattice polygons, inscribed in the unit cube, used to test the equations for the exact mean overcrossing number. (The networks have the same size and anisometry, but they can be distinguished by measuring their entanglements. For clarity, the *x*,*y*,*z*-labels for the coordinate axes are indicated only in example I.)

overcrossing number due to two perpendicular bonds separated by one lattice spacing. The bonds C_1 and C_3 in example II represent one such case (here, displaced along the *y*-direction). Using eq 23 with $b = 1$, we obtain immediately

$$\overline{N}(C_1,C_3) = \frac{1}{4\pi}\arctan\left(\frac{1}{\sqrt{3}}\right) = \frac{1}{24} \qquad (25)$$

This result applies to every pair of overcrossing bonds in Figure 3. In example II, there are six distinct such pairs (C_i, C_j), $i < j$, namely (C_1,C_3), (C_1,C_5), (C_2,C_4), (C_2,C_6), (C_3,C_5), and (C_3,C_6). Using eqs 24 and 25, we obtain the total mean overcrossing number for the network in example II: $\overline{N} = 2(6 \times [1/24]) = 1/2$. The other examples in Figure 3 can be analyzed in a similar manner. Table 1 summarizes the analytical results for the mean overcrossing numbers and compares them with the direct numerical calculation. As it can be seen, the results are in good agreement, but the precision of the numerical results is rather limited. Note that our numerical computations are quite demanding, involving a total of 10^7 randomized projections for each example. In contrast, the analytical computation is very fast, requiring only the classification of bonds into perpendicular noncoplanar pairs, followed by a computation of distances and inverse trigonometric functions. Note, however, that the present formalism provides only an analytical expression for $\overline{N}$ and *not* for the probabilities A_N for observing an integer

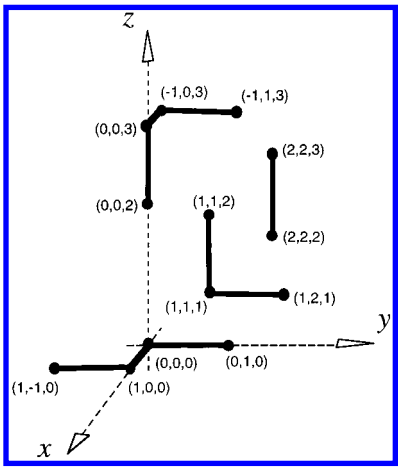

Figure 4. Example of a network in the cubic lattice exhibiting four maximum connected components. (The exact mean overcrossing number for this network is found to be $\overline{N} = 0.331\,686\,725\,225\,637\,947...$).

N number of overcrossings. The numerical results for these probabilities are listed in Table 1 for the examples in Figure 3. These A_N values give a more detailed description of the entanglements. (In addition, they explain why the precision of the numerical approach is larger for the network IV. In this latter case, the value $\overline{N} = 1$ is the result of *every* projection producing one and only one overcrossing, *i.e.*, $A_1 = 1$.)

As a final test, Figure 4 shows a more complicated network in the cubic lattice. This network is a "toy example" of the typical configurations produced when modeling polymer solutions or "melts" using lattice simulations.[47,48] This ensemble comprises four disjoint (maximum connected) components, determined by 13 nodes and nine bonds. The chosen coordinates are indicated in Figure 4. There are 21 pairs of nonconnected perpendicular bonds, although three of them are coplanar and do not contribute to overcrossings. Applying eq 23 to the remaining pairs and eq 19 for the total mean number of overcrossings, we obtain for the example in Figure 4:

$$\overline{N} = (2\pi)^{-1}\{-\arctan(2/\sqrt{6}) - 2\arctan(1/\sqrt{3}) + 3\arctan(4/3) + 2\arctan(3/\sqrt{17}) + \arctan(9/\sqrt{19}) - \arctan(3/2\sqrt{14}) - 2\arctan(6/\sqrt{14}) - 2\arctan(1/3\sqrt{11}) + 3\arctan(2/3\sqrt{14}) + \arctan(3/\sqrt{11})\} = 0.331\,686\,7... \qquad (26)$$

By averaging over 10 different series of 10^6 random projections,[16] a direct numerical calculation on this network produces $\overline{N} = 0.3318 \pm 0.0005$, in good agreement with (26). In this case, the only contributions to overcrossings

are $N \leq 3$, with probabilities given by $A_0 = 0.7435 \pm 0.0005$, $A_1 = 0.1952 \pm 0.0004$, $A_2 = 0.0474 \pm 0.0002$, and $A_3 = 0.0139 \pm 0.0001$. Other instantaneous configurations of any transient network can be computed in a similar fashion.

FURTHER COMMENTS AND CONCLUSIONS

In this work, we have presented the equations required for a precise, analytical computation of a geometrical measure of entanglement in a generic polymer network. The results generalize previous analyses, which had been restricted to closed polymers, knotted polymers, or linked pairs of polymers. Our basic equations (eqs 17−19) apply to an ensemble of possibly disjoint polymers, with maximum connected components of arbitrary topologies. The analysis remains the same, whether each connected component is a loop, a chain, a branched polymer, a dendrimer, or a combination of these. (In addition, the formalism can be extended to the case of two-dimensional, adsorbed polymers.[65]) The strength of our approach lies in the fact that the mean overcrossing number is reduced to a series of line integrals, each of which contains only a pair of bond−bond "crossings".

Since most standard simulations of random heteropolymers (including those of protein-like sequences) are performed as self-avoiding walks or directed walks in the cubic lattice,[45−50] our results in section 3 are particularly useful. It will be now possible to produce detailed characterization of molecular shape in model polymer solutions (or melts) in a fast, inexpensive manner.

Equation 19 can also be simplified, though to a smaller extent, in other three-dimensional lattices (*e.g.*, a diamond lattice). In addition, eq 19 can be given a closed form even for an off-lattice continuum, although the expression is very cumbersome. In this case, it may be more expedient to evaluate the integrals numerically.

The results in the previous section can also be applied to the analysis of *selected* types of overcrossings. For example, we can use the mean overcrossing number as a tool to describe the effect of *chain packing* on the entanglements. In this case, it may be useful to distinguish between the overcrossings due to two separate chains from the overcrossings within a chain. This can easily be done as follows. Let A and B be two maximum connected components ("chains") of the network, denoted as $A = \cup_{i=1} G_i$ and $B = \cup_{j=1} G_i$, where $A \cap B = \emptyset$. If $\overline{N}_{\text{inter}}$ stands for the mean overcrossing number due to bond−bond crossings *between* A and B, we have immediately

$$\overline{N}_{\text{inter}} = \overline{N}(A \cup B, A \cup B) - \overline{N}(A, A) - \overline{N}(B, B) \quad (27)$$

where the diagonal terms represent the self-overcrossings within each individual chain.

It should be mentioned that the present results can also be applied to the computation of other shape descriptors of entanglement. For instance, by removing the absolute value in the integrand of eq 19, we can compute the *average writhe* ($\bar{W}_r$) of the network instead of its mean overcrossing number.[9,19−24] The writhe associated with a given projection is the algebraic sum of the observed overcrossings, where right-handed crossings are given a handedness of "+1" and left-handed crossings are assigned "−1." Evidently, $\overline{N} \geq |\bar{W}_r|$. Both $\overline{N}$ and $\bar{W}_r$ provide useful information: in a *compact random configuration* we expect a large $\overline{N}$ and a vanishing $\bar{W}_r$, whereas in a configuration with *regular dihedral angles* (*e.g.*, a compact helix) we expect both $\overline{N}$ and $|\bar{W}_r|$ to be large. Conveniently, these two descriptors can be combined to produce a more effective shape characterization. For instance, a descriptor such as

$$\zeta = \frac{\overline{N} - |\bar{W}_r|}{\overline{N}} \quad (28)$$

can serve as *an order parameter*, because it exhibits two clear regimes: we expect $\zeta \sim 0$ in a nonentangled regular configuration and $\zeta \sim 1$ in an entangled random configuration. As a result, the parameter ζ may be useful for monitoring the occurrence of shape changes along configurational transitions, including those of "random coil → collapsed globule", "stretched chain → random coil", and "helix → random coil". The results in the present work will allow one to compute efficiently an order parameter for entanglements during the course of any of these transitions.

ACKNOWLEDGMENT

I thank Prof. A. Grosberg (MIT) for discussions, Prof. A. Kholodenko (Clemson) for sending a preprint of ref 37 prior to publication, and N. Grant (Laurentian) for her comments on the manuscript. This work has been supported by grants from FRUL (Laurentian University) and NSERC (Canada).

REFERENCES AND NOTES

(1) Doi, M.; Edwards, S. F. *The Theory of Polymer Dynamics*; Clarendon Press: Oxford, 1988.
(2) Strobl, G. R. *The Physics of Polymers*; Springer-Verlag: Berlin, 1996.
(3) de Gennes, P.-G. *Scaling Concepts in Polymer Physics*; Cornell University Press: Ithaca, 1985.
(4) Perkins, T; Smith, D. E.; Chu, S. *Science* **1994**, *264*, 819.
(5) Käs, J.; Strey, H.; Sackmann, E. *Nature* **1994**, *368*, 226.
(6) Käs, J.; Strey, H.; Tang, J.-X.; Finger, D.; Ezzell, R.; Sackmann, E.; Janmey, P. A. *Biophys. J.* **1996**, *70*, 609.
(7) Wasserman, S. A.; Cozzarelli, N. R. *Science* **1986**, *232*, 951.
(8) Bates, A. D.; Maxwell, A. *DNA Topology*; Oxford University Press: New York, 1993.
(9) Fuller, F. B. *Proc. Symp. Appl. Math.* **1962**, *14*, 64.
(10) White, J. H. *Am. J. Math.* **1969**, *91*, 693.
(11) Fuller, F. B. *Proc. Natl. Acad. Sci. U.S.A.* **1978**, *75*, 3557.
(12) Murasugi, K. *Knot Theory and Its Applications*; Birkhäuser: Boston, 1996.
(13) Mansfield, M. L. *Macromolecules* **1994**, *27*, 5924.
(14) Arteca, G. A.; Mezey, P. G. *Biopolymers* **1992**, *32*, 1609.
(15) Janse van Rensburg, E. J.; Sumners, D. W.; Wasserman, E.; Whittington, S. G. *J. Phys. A* **1992**, *25*, 6557.
(16) Arteca, G. A. *Biopolymers* **1993**, *33*, 1829.
(17) Arteca, G. A. *Int. J. Quantum Chem. QCS* **1994**, *28*, 433.
(18) Arteca, G. A. *J. Comput. Chem.* **1994**, *15*, 633.
(19) Lacher, R. C.; Sumners, D. W. In *Computer Simulation of Polymers*; Roe R. J., Ed.; Prentice-Hall: Englewood Cliffs, 1991.
(20) Janse van Rensburg, E. J.; Orlandini, E.; Sumners, D. W.; Tesi, M. C.; Whittington S. G. *J. Phys. A* **1993**, *26*, *L* 981.
(21) Orlandini, E.; Tesi, M. C.; Whittington, S. G.; Sumners, D. W.; Janse van Rensburg, E. J. *J. Phys. A* **1994**, *27*, L 333.
(22) Aldinger, J.; Klapper, I.; Tabor, M. *J. Knot Theory Ram.* **1995**, *4*, 343.
(23) Kholodenko, A. L.; Rolfsen, D. P. *J. Phys. A* **1996**, *29*, 5677.
(24) Moroz, J. D.; Kamien, R. D. *Nucl. Phys.* B **1997**, *506*, 695.
(25) Orlandini, E.; Tesi, M. C.; Janse van Rensburg, E. J.; Whittington, S. G. *J. Phys. A* **1997**, *30*, *L* 693.
(26) Moffatt, K. *Nature* **1990**, *347*, 367; **1996**, *384*, 114.
(27) O'Hara, J. *Topology* **1991**, *30*, 241.
(28) Freedman, M. H.; He, Z.-X.; Wang, Z. *Ann. Math.* **1994**, *139*, 1.

(29) Simon, J. In *Mathematical Approaches to Biomolecular Structure and Dynamics*; Mesirov, J. P., Schulten, K., Sumners, D. W., Eds.; Springer-Verlag: New York, 1996.
(30) Diao, Y.; Ernst, C.; Janse van Rensburg, E. J. *J. Knot Theory Ram.* **1997**, *6*, 633.
(31) Diao, Y.; Ernst, C.; Janse van Rensburg, E. J. *J. Knot Theory Ram.* **1997**, *6*, 799.
(32) Stasiak, A.; Katritch, V.; Bednar, J.; Michoud, D.; Dubochet, J. *Nature* **1996**, *384*, 122.
(33) (a) Katritch, V.; Bednar, J.; Michoud, D.; Scharein, R. G.; Dubochet, J.; Stasiak, A. *Nature* **1996**, *384*, 142. (b) Vologodskii, A. V.; Crisona, N. J.; Laurie, B.; Pieranski, P.; Katritch, V.; Dubochet, J.; Stasiak, A. *J. Mol. Biol.* **1998**, *278*, 1.
(34) Grosberg, A. Yu.; Feigel, A.; Rabin, Y. *Phys. Rev. E* **1996**, *54*, 6618.
(35) Janse van Rensburg, E. J.; Orlandini, E.; Sumners, D. W.; Tesi, M. C.; Whittington, S. G. *J. Knot Theory Ram.* **1997**, *6*, 31.
(36) Arteca, G. A. *Phys. Rev. E* **1994**, *49*, 2417; **1995**, *51*, 2600; **1997**, *56*, 4516.
(37) Kholodenko, A. L. ; Vilgis, T. A. *Phys. Rep.* **1998**, *298*, 251.
(38) Cantarella, J.; Kusher, R. B.; Sullivan, J. M. *Nature* **1998**, *392*, 237.
(39) Buck, G. *Nature* **1998**, *392*, 238.
(40) Arteca, G. A. *Biopolymers* **1995**, *35*, 393.
(41) Arteca, G. A. *Macromolecules* **1996**, *29*, 7594.
(42) Arteca, G. A. *J. Phys. Chem. B* **1997**, *101*, 4097.
(43) Arteca, G. A.; Caughill, D. I. *Can. J. Chem.* **1998**, *76*, 1402.
(44) Arteca, G. A.; Velázquez, I.; Reimann, C. T.; Tapia, O. *Phys. Rev. E* **1999** In press.
(45) Madras, N.; Slade, G. *The Self-Avoiding Walk*; Birkhäuser: Boston, 1996.
(46) Sokal, A. D. *Monte Carlo and Molecular Dynamics Simulations* in *Polymer Science*; Binder, K., Ed.; Oxford University Press: New York, 1995.
(47) Kremer, K.; Binder, K. *Comp. Phys. Rep.* **1988**, *7*, 259.
(48) Kremer, K.; Grest, G. S. *Monte Carlo and Molecular Dynamics Simulations in Polymer Science*; Binder, K., Ed.; Oxford University Press: New York, 1995.
(49) Sali, A.; Shakhnovich, E.; Karplus, M. *Nature* **1994**, *369*, 248.
(50) Abkevich, V. I.; Gutin, A. M.; Shakhnovich, E. *J. Mol. Biol.* **1995**, *252*, 460.
(51) Gauss, C. F. *König. Ges. Wiss. Göttingen* **1877**, *5*, 602.
(52) Câlugâreanu, G. *Rev. Math. Pure Appl.* **1959**, *4*, 5.
(53) Edwards, S. F. *Proc. R. Soc. (London)* **1967**, *91*, 513; *J. Phys. A* **1968**, *1*, 15.
(54) Brereton, M. G.; Shah, S. *J. Phys. A* **1981**, *14*, L 51.
(55) Wiegel, F. W. *Phase Transitions and Critical Phenomena*; Domb, C., Lebowitz, J. L. Eds.; Academic Press: London, 1983; vol. 7.
(56) Brereton, M. G. *J. Mol. Struct. Theochem.* **1995**, *336*, 191.
(57) Kleinert, H. *Path Integrals in Quantum Mechanics, Statistics, and Polymer Physics*; World Scientific: Singapore, 1995.
(58) O'Neill, B. *Elementary Differential Geometry*; Academic Press: Boston, 1966; p 290.
(59) Arnol'd, V. I. *Sel. Math. Sov.* **1986**, *5*, 327.
(60) Freedman, M. E.; He, Z.-X. *Ann. Math.* **1991**, *134*, 189.
(61) Brynson, S.; Freedman, M. E.; He, Z.-X.; Wang, Z. *Bull. Am. Math. Soc. (NS)* **1993**, *28*, 99.
(62) Ozol'-Kalnin, V.G. *Pis'ma Zh. Eksp. Teor. Fiz.* **1994**, *59*, 535. [*JETP Lett.* **1994**, *59*, 565.]
(63) Berger, M.; Gostiaux, B. *Géométrie Differentielle: Variétés, Courbes et Surfaces [Differential Geometry: Manifolds, Curves, and Surfaces]*; Presses Universitaires de France: Paris, 1987; p 283.
(64) Gradshtein, I. S.; Ryzhik, I. M. *Tablitsy Integralov, Summ, Riadov i Proizvedenii [Tables of Integrals, sums, series, and products]*; FM Publishers: Moscow, 1962.
(65) Arteca, G. A.; Zhang, S. *Phys. Rev. E* **1999**, *59*, 4203.

CI980144L